https://doi.org/10.5194/egusphere-2022-742
Preprint. Discussion started: 9 September 2022

Effects of fire danger indexes and land cover on fire growth in Peru

Harry Podschwit[1], William Jolly[1], Ernesto Alvarado[2], Andrea Markos[3], Satyam Verma[2], Sebastian Barreto-Rivera[3], Catherine Tobón-Cruz[3], and Blanca Ponce-Vigo[3]

[1]US Forest Service, Rocky Mountain Research Station, Fire Sciences Laboratory, 5775 Highway 10 West, Missoula, MT, USA
[2]School of Environmental and Forest Sciences, University of Washington, Seattle, USA
[3]US Forest Service, International Programs, 1 Thomas Circle, NW Suite 400 Washington D.C., U.S.A.

Correspondence: Harry Podschwit (hpodschwit@gmail.com)

Abstract. Statistical analyses of wildfire growth are rarely undertaken, particularly in South America. In this study, we describe a simple and intuitive difference equation model of wildfire growth that uses a spread parameter to control the radial speed of the modeled fire and an extinguish parameter to control the rate at which the burning perimeter becomes inactive. Using data from the GlobFire project, we estimate these two parameters for 1003 large, multi-day fires in Peru between 2001 and 2020. For four fire-prone ecoregions within Peru, a set of 18 generalized linear models are fit for each parameter that use fire danger indexes and land cover covariates. Akaike weights are used to identify the best-approximating model and quantify model uncertainty. We find that, in most cases, increased spread rates and extinguish rates are positively associated with fire danger indexes. When fire danger indexes are included in the models, the spread component is usually the best choice. We also find that forest cover is negatively associated with spread rates and extinguish rates in tropical forests, and that anthropogenic cover is negatively associated with spread rates in xeric ecoregions. We explore potential applications of this model to wildfire risk assessment and burned area forecasting.

1 Introduction

Although researchers frequently characterize fire in terms of size (Doerr and Santín, 2016), there are a number of other parameters that describe unique dimensions of fire behavior. For instance, spread rates are an important parameter for understanding fire entrapment and burnover risks. When spread rates are low, nearby individuals have more time to detect and escape an advancing fire front than when spread rates are high (Page et al., 2019). Indeed, unexpected and explosive fire growth has been implicated in a large number of fatal wildfires (Viegas and Simeoni, 2011) and rarely prescribed fire (Twidwell et al., 2015) accidents. For this reason, numerous models (Sullivan, 2009b, a), policies (Butler, 2014), technologies (De Vivo et al., 2021), and tools (Jolly et al., 2019) have been developed to mitigate the risk of high-spread events to firefighters and the general public. Fire spread rates are also an informative parameter for understanding firefighting effectiveness (Rapp et al., 2021; Finney et al., 2009). In addition to fire spread, descriptions of how and when the length of the burning perimeters reduce over time can be valuable to decision makers. Much of the research deals with this topic indirectly by focusing on extinguishment in terms of fireline production rates (Fried and Fried, 1996). However, the length of burning perimeter may be reduced for reasons unre-

https://doi.org/10.5194/egusphere-2022-742
Preprint. Discussion started: 9 September 2022

lated to fire suppression, and less often are these other factors explored. The burning perimeter may be reduced when a portion of the fire front spreads into a preexisting fuel break such as previously burned areas, waterbodies, roads, and inflammable vegetation (Reed and McKelvey, 2002). Moreover, local weather may differentially control fire spread and extinguishment, leading to scenarios where one portion of a fire may be spreading at the same time another portion is dying out (Price et al., 2014; Reed and McKelvey, 2002). A better understanding of the dynamics and relevant factors mediating fire extinguishment is important because it can improve fire-related decisions by reducing redundancies in fireline construction strategies (Wei et al., 2021), and improve the cost-effectiveness of firefighting (Houtman et al., 2013).

At least part of the reason that fire parameters such as spread and extinguish rates are overlooked by researchers is that the relevant data are uncommon. Daily fire growth data are rare, usually coming from case studies and administrative records (Taylor et al., 2013), and although fire perimeter data are occasionally available (Zhong et al., 2016), identifying which portions of the perimeter are active and inactive can be a difficult task (Anderson et al., 2009). Where these data are available, they are subject to fairly high levels of uncertainty and often contain gaps and errors (Podschwit et al., 2018; Kolden and Weisberg, 2007). These problems are particularly noticeable in locations that lack the historical records and technological resources that are more commonly found in the United States, Canada, and Australia. In South America, data regarding fire spread rates are available from a few experimental studies (Ray et al., 2005; Bufacchi et al., 2017), but these estimates may not be representative of the real-world conditions (Melcher et al., 2016) and cannot be reliably extrapolated to other locations. In most cases, information about real-world fire spread and extinguishment must be derived from satellite data (Andela et al., 2019).

In spite of these problems with data quantity and quality, we can use available research to develop some intuition regarding which environmental factors are likely to be relevant to Peruvian fire spread and extinguishment. The risk of firefighter entrapments in the United States are typically associated with rapid fire spread (Page et al., 2019), and this fire parameter is both directly (Rapp et al., 2021) and indirectly (Jolly et al., 2019) associated with low fuel moisture and anomalously high wind speed. Existing conceptual climate-fire models can also inform us how fuel availability and flammability are likely to mediate fire spread in different Peruvian environments. Ecosystems that have abundant fuel available (e.g. forests) are often climate-limited and require exceptionally dry periods to permit large fire growth. On the other hand, ecosystems that are frequently dry typically have low levels of fuel (e.g. grasslands), and unlike climate-limited ecosystems require above-average antecedent precipitation to produce fuel loads of sufficient quantity and continuity to permit large fire growth (Meyn et al., 2007). Indeed, naturally occurring large fires in the Amazon - an unambiguously climate-limited ecosystem - are very rare (Lima et al., 2012) and are largely thought to be mediated by ambient humidity levels (Cochrane, 2003). When fire does occur in the Amazon, they are usually intentionally set to clear forest for agriculture (Cochrane, 2003) and are characterized by low spread rates ($\ll 1$ m/min) and low flame height (< 0.5 m) (Cochrane, 2003; Ray et al., 2005; Bufacchi et al., 2017). In the Peruvian Andes - an ecoregion that is largely unforested - precipitation patterns follow a sawtooth pattern during peak fire years, where precipitation is anomalously high in the year previous, followed by dry weather during the peak fire year (All et al., 2017). Similarly, ENSO-related increases in precipitation in the Sechura desert of northern Peru are associated with increased fuel loads and subsequent increases in fire activity (Block et al., 2000). Satellite-derived estimates of fire spread can also provide intuition regarding the scale and variability of fire spread in Peru. The typical areal changes in fire is estimated to be less than 2 km^2

https://doi.org/10.5194/egusphere-2022-742
Preprint. Discussion started: 9 September 2022

per day in South America. These growth estimates do not strongly vary within South America, but large differences are found between xeric regions versus humid tropical regions globally (Andela et al., 2019).

Given that meteorology and land cover are known to be important influences on fire spread in other locations, we would like to explore the relevance of these factors to fire spread in Peru, where these relationships have not been well quantified. To do this, we will develop a simple difference equation model to summarize satellite-derived fire growth data. We will then build regression models to predict the difference equation parameters and determine if a suite of meteorological and land cover covariates are statistically significant predictors. The intended outcome of this analysis is to present a relatively simple method of predicting fire growth based on environmental conditions that can be applied nearly anywhere globally.

2 Model

The difference equation model begins with two simplifying assumptions regarding fire growth:

1. Fire spreads at a constant rate, r, from all angles from an ignition point.
2. After the first time step, a constant length, l, of the fire's perimeter is extinguished.

A graphical description of these dynamics for various values of r and l is shown below (Figure 1). Note that in this study the word "growth" is reserved to describe areal changes in fire and "spread" is reserved to describe radial changes in fire.

2.1 Sector length and arc

We hereafter assume that r and l are measured in kilometers per day. It follows from these assumptions that on the first day, the fire is a circle with a radius of r km and $2\pi r$ km of initial burning perimeter. There is no extinguishment of burning perimeter on the first day. On the second day the amount of burning perimeter is reduced by l km and the fire continues to spread radially at rate r km/day. For any $l \geq 2\pi r$, there is no fire growth on the second day since all of the burning perimeter is extinguished. The sector arc of burning perimeter at the start of the second day is calculated via (Equation 1).

$$\theta_2 = \frac{\max(2\pi r - l, 0)}{r}. \tag{1}$$

The second day's final burning perimeter length is calculated from (Equation 2)

$$S_2 = \theta_2 \times (2r); \tag{2}$$

and in general, we can calculate the current burning perimeter length using (Equation 3).

$$S_t = \theta_t \times (tr). \tag{3}$$

https://doi.org/10.5194/egusphere-2022-742
Preprint. Discussion started: 9 September 2022

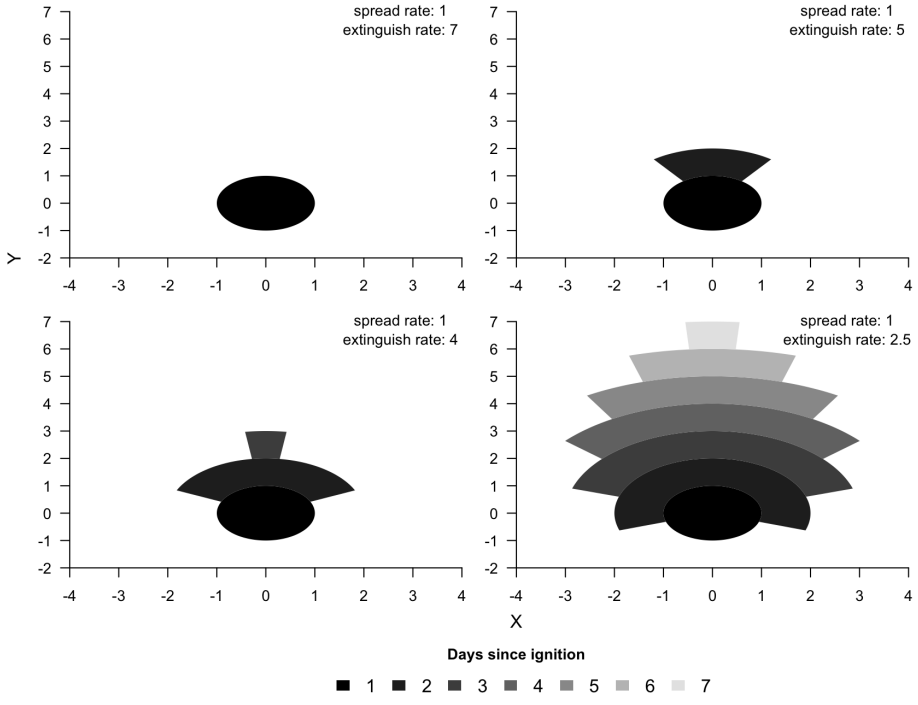

Figure 1. Graphical depiction of modeled fire growth for four pairs of spread rate and extinguish rate parameters. The X and Y dimension represent the distance from the ignition point at an arbitrary scale.

Moreover, since the sector arc is calculated by taking the sector length and dividing by the radius, we can see that the sector arc follows (Equation 4).

$$\theta_t = \frac{\max\left(S_{t-1} - l, 0\right)}{r(t-1)}. \tag{4}$$

We can now use (Equation 3) to greatly simplify (Equation 4). Namely, if $t > 1$, then

$$\theta_t = \frac{\max\left(\theta_{t-1}(t-1)r - l, 0\right)}{r(t-1)}. \tag{5}$$

If we assume that the fire is not going to be extinguished at time t, then $S_{t-1} \geq l$ and (Equation 5) may be further simplified into the following difference equation (Equation 6).

$$\theta_t = \theta_{t-1} - \frac{l}{r(t-1)}. \tag{6}$$

https://doi.org/10.5194/egusphere-2022-742
Preprint. Discussion started: 9 September 2022

An exact solution to the difference equation is produced by noting,

$$\Delta\theta_t = \theta_t - \theta_{t-1} = -\frac{l}{r(t-1)}. \tag{7}$$

And that for $t > 1$,

$$\theta_t = \theta_1 + \sum_{n=2}^{t} \Delta\theta_n = \theta_1 - \frac{l}{r}\sum_{n=2}^{t}\frac{1}{(n-1)} = \theta_1 - \frac{l}{r}H_{t-1}, \tag{8}$$

where H_{t-1} is a harmonic series.

2.2 Area and duration

The equation representing the burning perimeter can be manipulated to represent more commonly used wildfire parameters such as area and duration. Cumulative burn area over time can be calculated by noting that each day's growth can be represented as a partial annulus (Figure 1, Equation 9) and taking the sum of these daily growth predictions (Equation 10).

$$\Delta A_t = A_t - A_{t-1} = \frac{\theta_{t-1}}{2} \times [(t \times r)^2 - ((t-1) \times r)^2]. \tag{9}$$

$$A_t = \sum_{n=1}^{\infty} \Delta A_t = \frac{r^2}{2}\sum_{n=1}^{\infty}\theta_{n-1} \times (n^2 - (n-1)^2) = \frac{r^2}{2}\sum_{n=1}^{\infty}\theta_{n-1} \times (2n-1). \tag{10}$$

In practice, only a partial series is required because the fire will cease to grow at some point in time. The number of days from ignition until wildfire growth ceases can be derived from (Equation 8) and we can see that the modeled fire will grow for all t such that $\frac{\theta_1 r}{l} > H_{t-1}$.

2.3 Estimation of model parameters from area and duration

Note in (Equation 8) that if the day 1 burning arc, θ_1, is known, then the dynamics of the burning arc are entirely determined by the ratio of the spread and extinguish rates, $\gamma = \frac{l}{r}$, a quantity we hereafter refer to as the relative decay rate. Hence, if a burned area time series with area (A) and duration (T) was desired, then estimates of the spread rate $\hat{r}$ and extinguish rate $\hat{l}$ could be obtained by choosing a $\hat{\gamma}$ such that,

$$\frac{\theta_1}{H_T} \leq \hat{\gamma} < \frac{\theta_1}{H_{T-1}}. \tag{11}$$

Next, a normalizing factor, c, is estimated (Equation 12), which assumes $\hat{\gamma}$ and an initial spread rate of $r = 1$.

$$c = \frac{1}{2}\sum_{n=1}^{T}\theta_{n-1|\gamma=\hat{\gamma}} \times (2n-1). \tag{12}$$

https://doi.org/10.5194/egusphere-2022-742
Preprint. Discussion started: 9 September 2022

An estimate of $\hat{r}$ is then obtained via,

$$\hat{r} = \sqrt{\frac{A}{c}}. \tag{13}$$

The difference equation produced from $\hat{r}$ and $\hat{l} = \hat{r}\hat{\gamma}$ will have duration T and final area A.

3 Application

3.1 Data and preprocessing

GlobFire data (Artés et al., 2019) were clipped to boundaries of Peru, and disaggregated into four ecoregions as defined from the Nature Conservancy[1]. Each ecoregion is approximately similar in terms of climate and vegetation. Regional variability in fire detection probabilities were lessened by limiting our study to large and long duration events, which are likely to be detected regardless of forest cover and atmospheric conditions. Hence, incidents that were smaller than 405 hectares or incidents that reportedly burned for one day were removed from the analysis. The spatially explicit growth maps produced from GlobFire were converted into spatially-inexplicit burned area time series and the centroid of the final perimeter recorded. Summary statistics of the incidents disaggregated by ecoregion are reported in (Table 1) and a map of the incident locations is shown in (Figure 2).

Table 1. Regional sample size plus quartiles for both fire size (km^2) and duration (days)

Ecoregion	**Sample size**	**Size**					**Duration**				
		Min	Q_1	Q_2	Q_3	Max	Min	Q_1	Q_2	Q_3	Max
Xeric	38	4.13	4.81	5.96	9.51	65.70	2	5	8	10	21
Andean	252	4.11	4.83	6.49	10.76	69.33	2	5	6	9	24
Dry forest	50	4.25	5.01	7.09	14.50	289.44	3	5	7	10.75	18
Amazon	663	4.14	4.88	6.34	9.05	91.52	2	7	9	13	40

Five fire danger indexes (FDIs) are calculated using ERA5 reanalysis for 2001-2020[2]: the burning index (BI), energy release component (ERC), spread component (SC) (Bradshaw et al., 1984), fire weather index (FWI), and the Keetch-Byram Drought Index (KBDI) (Littell et al., 2016). The raw values were converted into a score by subtracting the mean and dividing by the standard deviation calculated from 2001-2020 data. Additionally, land cover data came from the GlobCover dataset[3].

The FDI values for each incident were extracted on the reported ignition date of the fire and at the incident centroid. The number of pixels within the final burn perimeter from each land cover type was recorded, reclassified using (Table 2), and converted into percentages.

[1] https://geospatial.tnc.org/datasets/b1636d640ede4d6ca8f5e369f2dc368b/about
[2] https://www.wfas.net/data/SAR/
[3] http://due.esrin.esa.int/page_globcover.php

https://doi.org/10.5194/egusphere-2022-742
Preprint. Discussion started: 9 September 2022

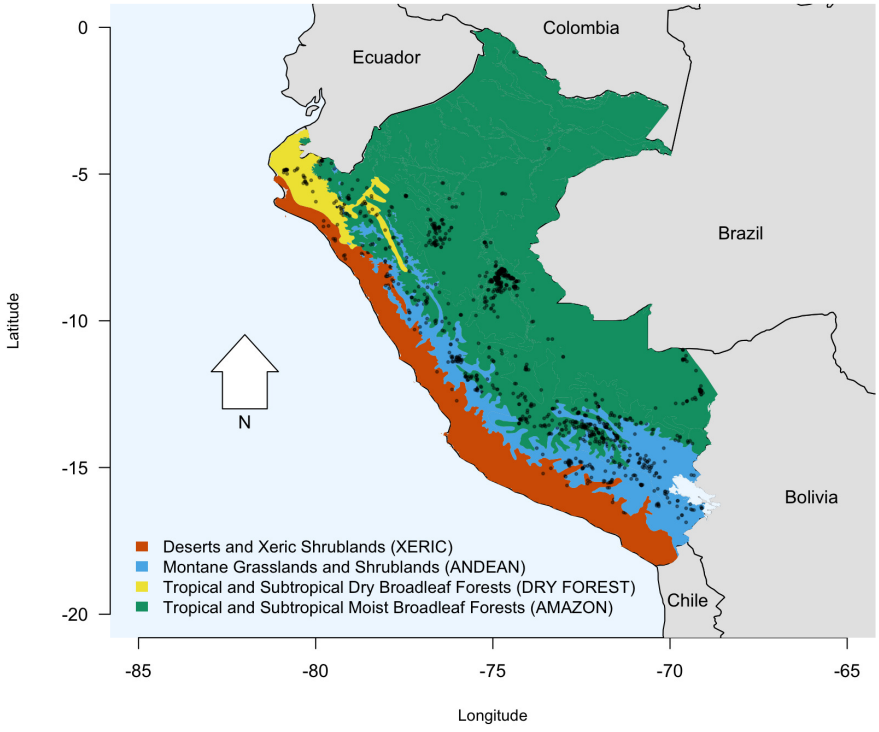

Figure 2. Map of the Peruvian ecoregions considered in this study with 2001-2020 GlobFire centroids of large, multi-day fires overlaid.

Table 2. Reclassification of GlobCover data

GlobCover value	New value
Post-flooding or irrigated croplands (or aquatic)	Anthropogenic
Mosaic cropland (50-70%) vegetation (grassland/shrubland/forest) (20-50%)	
Mosaic vegetation (grassland/shrubland/forest) (50-70%) / cropland (20-50%)	
Artificial surfaces and associated areas (Urban areas >50%)	
Closed to open (>15%) broadleaved evergreen or semi-deciduous forest (>5m)	Forest
Closed (>40%) broadleaved deciduous forest (>5m)	
Open (15-40%) broadleaved deciduous forest/woodland (>5m)	
Closed (>40%) needleleaved evergreen forest (>5m)	
Closed to open (>15%) broadleaved forest regularly flooded - Fresh or brackish water	
Closed (>40%) broadleaved forest or shrubland permanently flooded - Saline or brackish water	

https://doi.org/10.5194/egusphere-2022-742
Preprint. Discussion started: 9 September 2022

3.2 Estimation of model parameters

For each incident, the spread rate (r) and the extinguish rate (l) are estimated using the burned area time series derived from GlobFire. Specifically, for each burned area time series, the values of r and l that minimized the root mean square error (RMSE) were identified using the Nelder-Mead optimization algorithm (Nelder and Mead, 1965). To increase the likelihood that the global optimum was identified, 1000 initial best guesses of the model parameters were obtained by using a normal distribution with standard deviation one to jitter the estimates produced with the methods described in section 2.3. The optimization routine was run for each of the 1000 best guesses and the run producing the lowest root mean square error was assumed to be the global optimum. The correlation of these two parameters was explored using two methods. Firstly, the spearman correlations of the spread rate and extinguish rates estimates were calculated for each ecoregion. Secondly, a quadratic model that predicted the extinguish rate from the spread rate was fit using least-squares regression.

3.3 Statistical modeling

An initial set of 18 generalized linear models were considered for each ecoregion and model parameter. The 18 candidates were produced by considering all linear combinations of FDIs and land cover covariates such that at most one variable from each variable category was used. The generalized linear model assumed a inverse-link and Gamma density function. The validity of the Gamma density function was verified via visual inspection of Q-Q plots with a 95% simultaneous confidence band as calculated from the *distrMod* package (Computing et al., 2013). The best models were selected using Akaike weights (Wagenmakers and Farrell, 2004), which represent the probability that a model candidate was the true best-approximating model from the original set of 18 models. Akaike weights are calculated from a commonly used model selection criterion, Akaike information criterion (AIC), but has the added benefit of gauging the level of model uncertainty with probabilities, which are easier to interpret than the raw AIC values. All calculations of this analysis were performed in the R programming environment (Computing et al., 2013).

3.4 Results

3.5 Difference equation parameters and performance

The rate at which fires spread and are extinguished varied by ecoregion . The mean spread rates were highest in the Andean and dry forest ecoregions, and was lowest in the Amazon ecoregion. The mean extinguish rate was highest in the dry forest ecoregion and lowest in the Amazon ecoregion (Figure 3). The gamma distribution provided a high-quality parametric approximation of the distribution of observed spread rates (Appendix A1) and a slightly lower quality approximation of the distribution of extinguish rates (Appendix B1).

The spread rate and extinguish rate were highly correlated with one another. Spearman correlation coefficients ranged from 0.91 in the dry forest ecoregion to 0.96 in the Amazon and Xeric ecoregions. The observed relationship between the two parameters was well-described using a quadratic model (Figure 4).

https://doi.org/10.5194/egusphere-2022-742
Preprint. Discussion started: 9 September 2022

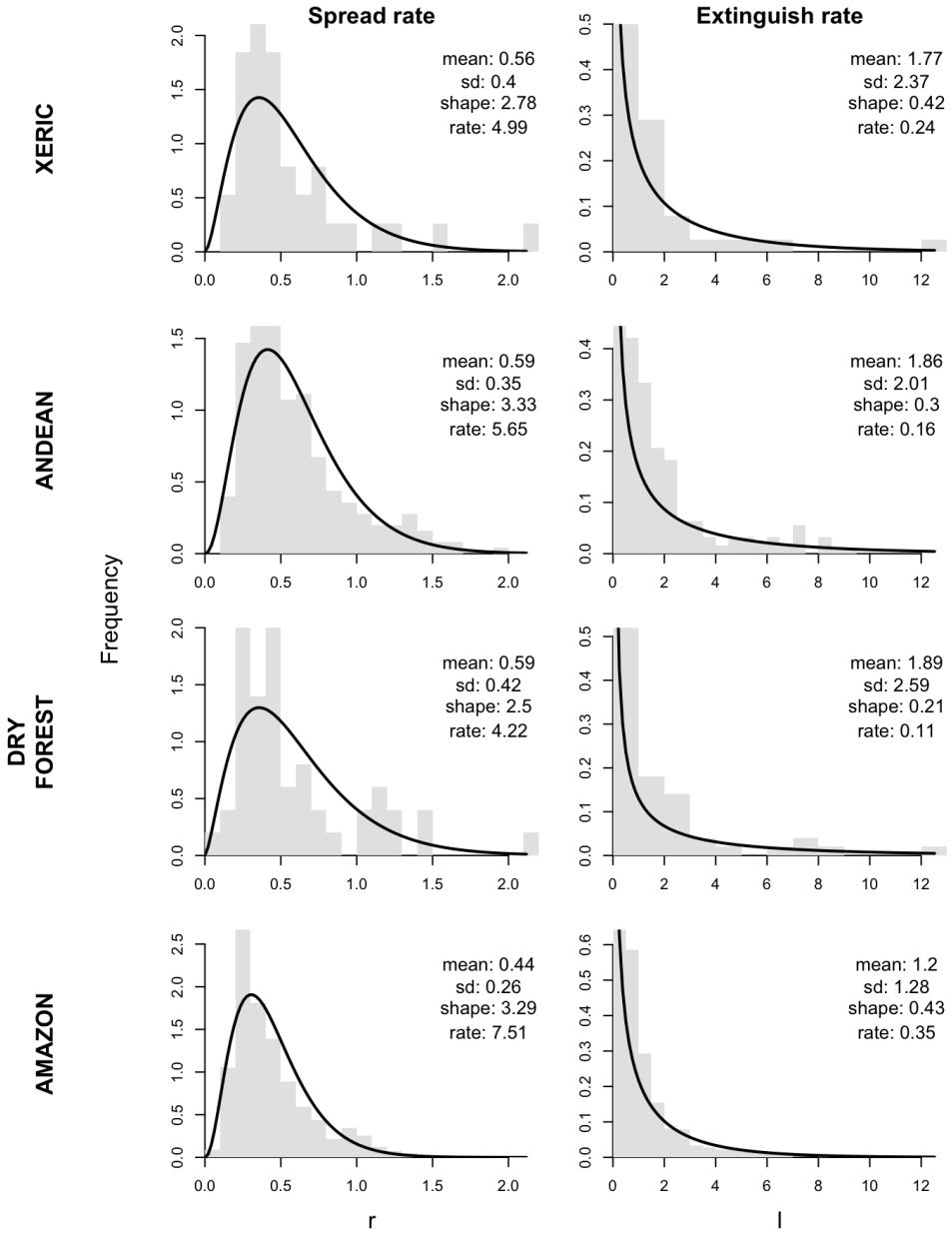

Figure 3. Histograms of the spread rates and extinguish rates (in kilometers per day) disaggregated by ecoregion. Maximum-likelihood estimates of the gamma distribution are overlaid. The mean, standard deviation, estimated shape, and estimated rate parameters are reported in the upper right of each panel.

165 The difference equation model well-approximated the observed daily growth of the burned area time series across all ecoregions. The lowest median RMSE (0.54 km^2) was seen in xeric ecoregion, whereas the highest median RMSE was seen in dry

https://doi.org/10.5194/egusphere-2022-742
Preprint. Discussion started: 9 September 2022

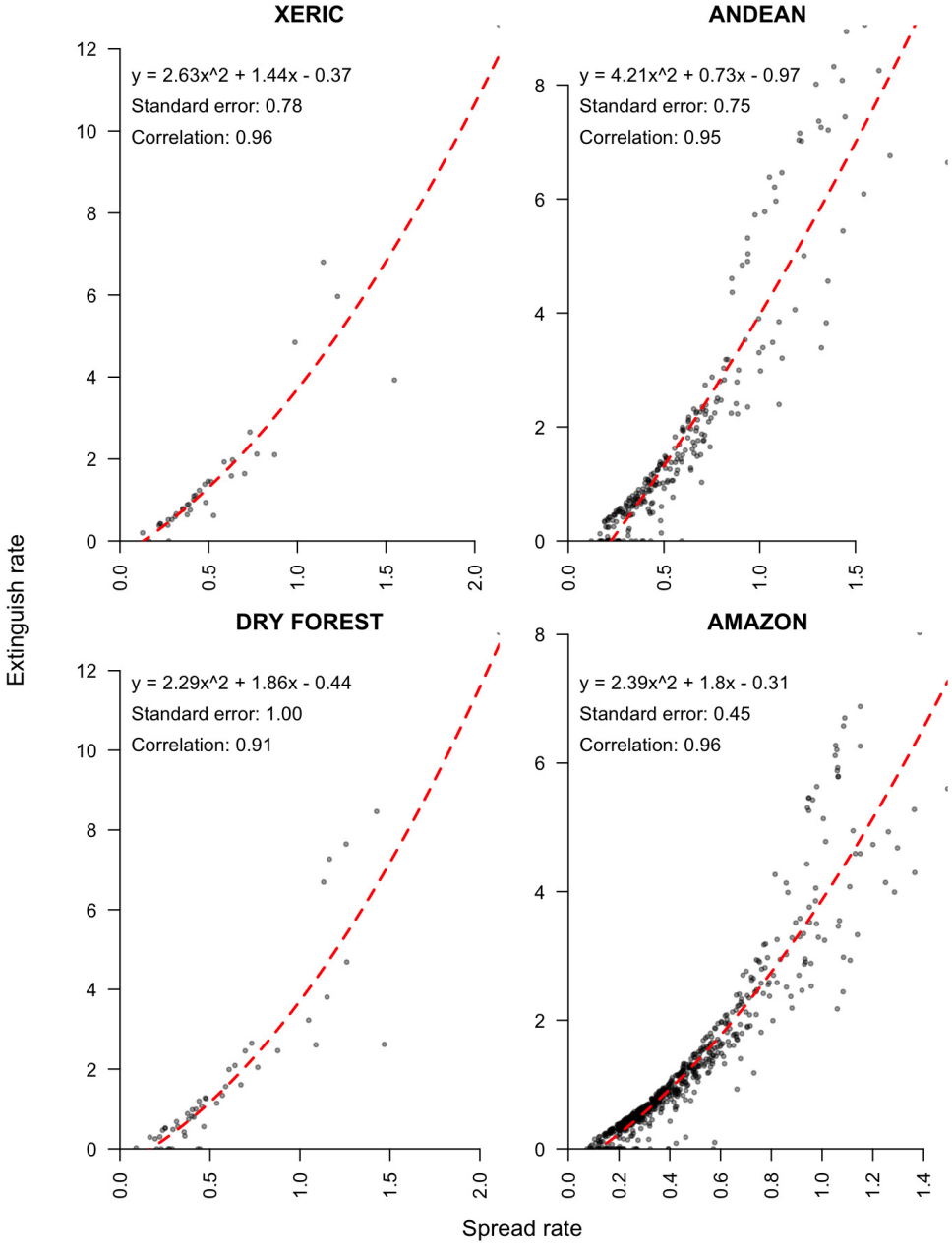

Figure 4. Scatterplots of observed relationship between spread rate and extinguish rate (in kilometers) disaggregated by ecoregion. Least-squares fit of quadratic model and spearman correlation coefficient are reported in upper left of each panel.

forests (0.76 km^2). The difference equation model did particularly well on fires smaller than 10 km^2 and fires less than three weeks in duration (Figure 5), which were characteristic of the majority of wildfire observations in this study (Table 1).

https://doi.org/10.5194/egusphere-2022-742
Preprint. Discussion started: 9 September 2022

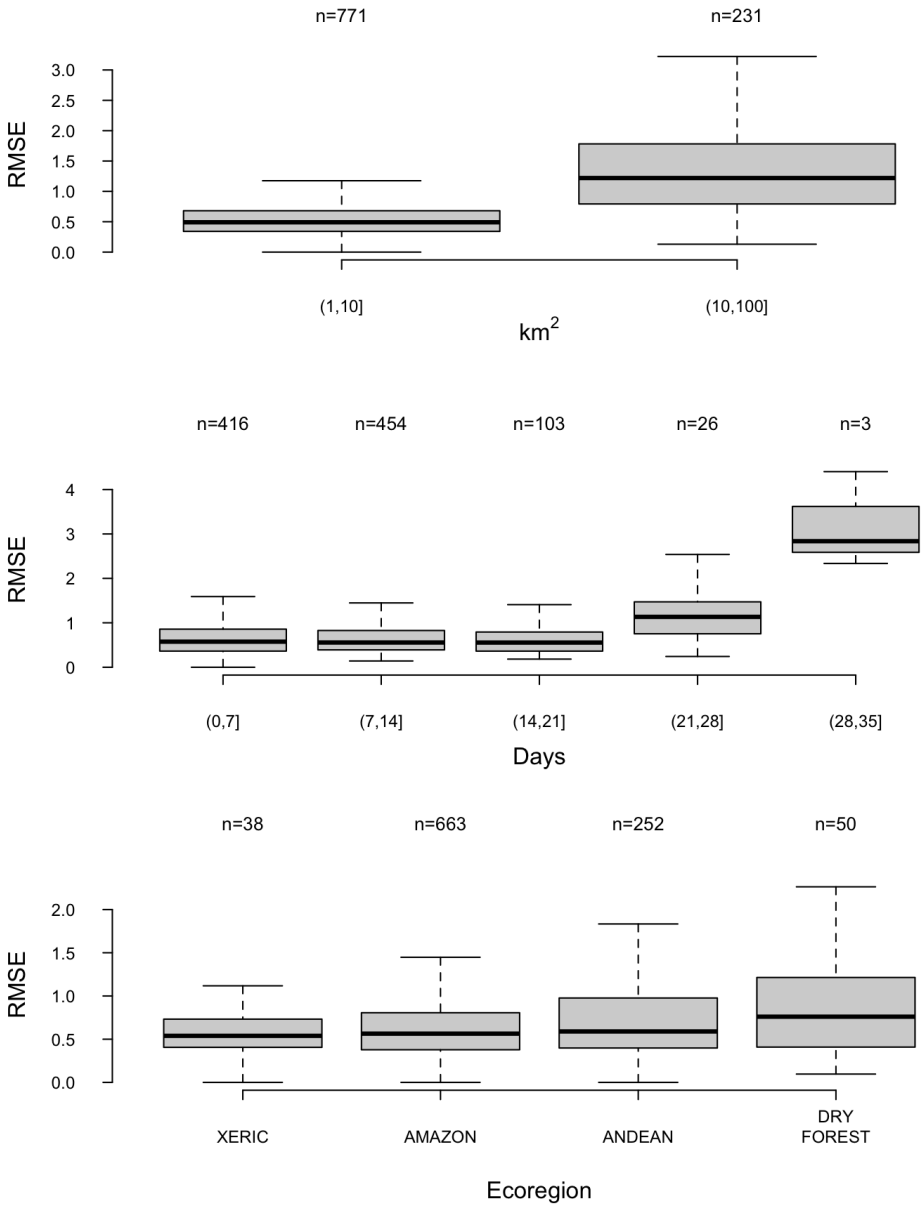

Figure 5. Boxplots of root-mean square error estimates calculated from best-fit difference equation predictions and GlobFire observations. Root-mean square error estimates are disaggregated by size, duration, and ecoregion. Sample size is reported above the boxplots and outliers have been removed for visualization purposes.

https://doi.org/10.5194/egusphere-2022-742
Preprint. Discussion started: 9 September 2022

3.6 Best-fitting parameter models

In the xeric ecoregion, the best-approximating model of spread rates predicted that fire would grow faster as FWI increased and as the percent of anthropogenic cover decreased, but the relationships were only weakly statistically significant. A strongly significant positive relationship between fire spread and the SC was observed in the best-approximating Andean spread model. The best-approximating spread model in the dry forest ecoregion did not include any FDI or land cover variables. In the Amazon ecoregion, the best-approximating model of spread assumed a positive relationship with SC and negative relationship with percent forest land cover, both covariates were very-strongly significant (Table 3).

Table 3. Summary of spread parameter generalized linear models for each ecoregion. Summary including formula, Akaike weight, and significance level. P-values greater than 0.10 are interpreted as not significant (ns), P-values less than 0.1 are interpreted as weakly significant (.), P-values less than 0.05 are interpreted as significant (*), P-values less than 0.01 are interpreted as strongly significant (**), and P-values less than 0.001 are interpreted as very-strongly significant (***).

Ecoregion	$-\frac{1}{\mu}$	**Dispersion**	**AIC weight**	**P-value**	
				FDI	**Land cover**
XERIC	$-1.87 + 0.20 \times FWI - 1.85 \times percent.anthro$	0.43	0.25	.	.
ANDEAN	$-1.85 + 0.16 \times SC$	0.33	0.29	**	
DRY FOREST	-1.68	0.50	0.16		
AMAZON	$-1.97 + 0.16 \times SC - 0.95 \times percent.forest$	0.31	0.97	***	***

In the xeric and dry forest ecoregions, the extinguish rate models did not include any covariates. In the Andean ecoregion, SC had a strongly significant and positive relationship with the extinguish rate. In the Amazon ecoregion, extinguish rates were predicted to increase with the increased SC and decreased forest cover; both covariates were very-strongly significant (Table 4).

Table 4. Summary of extinguish rate generalized linear models for each ecoregion. Summary including formula, Akaike weight, and significance level. P-values greater than 0.10 are interpreted as not significant (ns), P-values less than 0.1 are interpreted as weakly significant (.), P-values less than 0.05 are interpreted as significant (*), P-values less than 0.01 are interpreted as strongly significant (**), and P-values less than 0.001 are interpreted as very-strongly significant (***).

Ecoregion	$-\frac{1}{\mu}$	**Dispersion**	**AIC weight**	**P-value**	
				FDI	**Land cover**
XERIC	-0.56	1.79	0.14		
ANDEAN	$-0.62 + 0.08 \times SC$	1.16	0.12	**	
DRY FOREST	-0.53	1.87	0.18		
AMAZON	$-0.70 + 0.08 \times SC - 0.47 \times percent.forest$	1.11	0.50	***	***

https://doi.org/10.5194/egusphere-2022-742
Preprint. Discussion started: 9 September 2022

For the spread models, the Akaike weights - the probability that the true best-approximating model was selected from the 18 candidates - ranged from 0.16 in the dry forest ecoregion to 0.97 in the Amazon ecoregion (Table 3). For the extinguish rate models, this probability ranged from 0.12 in the Andean ecoregion to 0.50 in the Amazon ecoregion (Table 4). The probability that the true best-approximating spread model contained both a land cover and FDI covariate ranged was 0.32 in the dry forest ecoregion, 0.45 in the Andean ecoregion, 0.65 in the xeric ecoregion, and >0.99 in the Amazon. The probability that the true best-approximating extinguish model contained both a land cover and FDI covariate was lower, and ranged from 0.29 in the dry forest ecoregion, 0.36 in the Andean ecoregion, 0.38 in the xeric ecoregion, and 0.91 in the Amazon ecoregion (Figure 6).

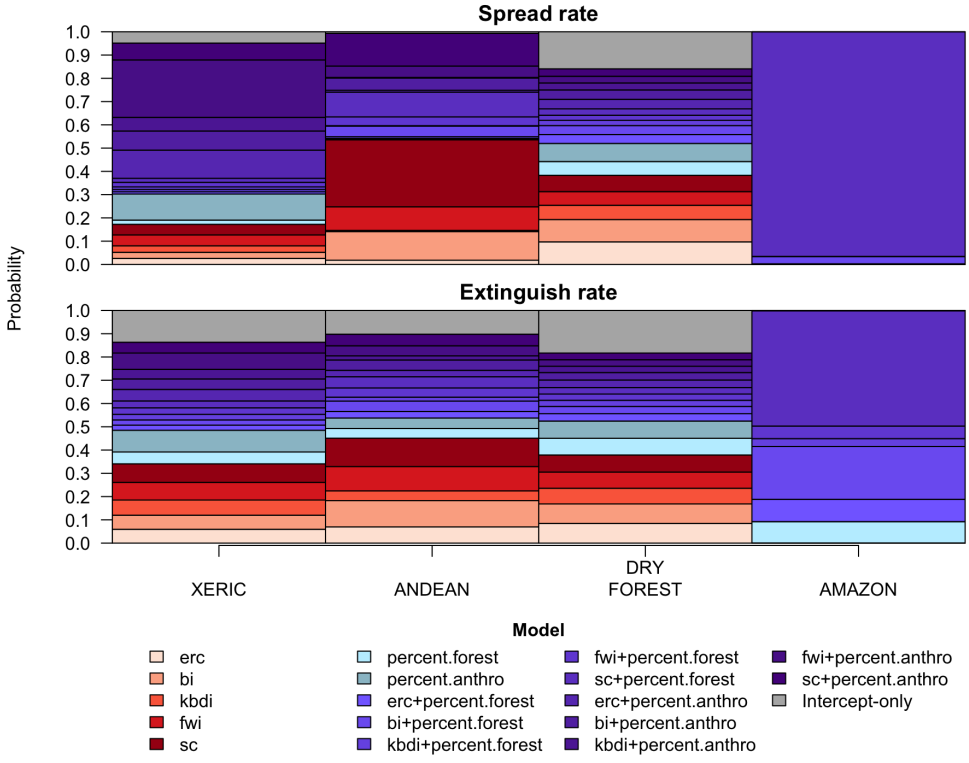

Figure 6. Barplots of Akaike weights - the probability that each model candidate is truly the best-approximating model - for each ecoregion and parameter. Models that contain both a FDI and land cover covariate are colored purple, those that contain only a FDI are colored red, those that only contain a land cover variable are colored blue, and the Intercept-only model are colored grey.

3.7 Expected growth curves

The effects of fire weather and land cover varied dramatically across ecoregions. In the xeric ecoregion, large FWI values were characterized with larger, faster growing, and longer duration fires compared to small FWI values. High anthropogenic cover was associated with much smaller, slower spreading, and shorter duration fires compared to areas with low anthropogenic cover. Changes in fire weather and land cover were predicted to have no effects on fire growth in the dry forest ecoregions.

https://doi.org/10.5194/egusphere-2022-742
Preprint. Discussion started: 9 September 2022

In the Andean ecoregion, increases in the SC tended to result in slightly larger and faster growing fires, but the expected fire duration was nominally smaller in the highest fire danger scenario considered. In the Amazon ecoregion, high SC values were characterized by increases in expected fire size and spread rate, and slight decreases in fire duration. Increases in forest cover were predicted to reduce fire size and spread rates, and increase fire duration (Figure 7).

4 Discussion

4.1 Difference equation validity

All models are approximations of the real world, and the relevant question to ask is whether the models can provide useful information (Anderson and Burnham, 2004). With this in mind, we argue that the difference equation model presented in this paper has a number of advantages over other approaches used to model fire growth. Firstly, this model is simple, requiring estimation of only a few parameters. This model is therefore vastly easier to implement than other commonly used spread models that require complex data inputs and subjective decisions regarding initialization parameters (Sullivan, 2009b, a). The model parameters are also easily interpreted and are directly related to the underlying fire processes. Although alternative difference equation models exist that could adequately represent observed fire growth, (Podschwit et al., 2018), the interpretation of the model parameters in these alternative models is cumbersome because they were not originally developed to represent fire growth.

Most importantly, these difference equations well-approximated observed fire growth data (Figure 5). Although performance deteriorated in larger, longer-duration fires, this tendency is not unique to this model (Podschwit et al., 2018), and additional parameters or covariates could be included to improve the goodness-of-fit in these cases. The fact that the spatial distribution of predicted spread rates conformed to previously known patterns of fire spread adds to the credibility of these models. Specifically, that the lowest spread parameter rates were observed in the Amazon ecoregion is largely consistent with existing research (Ray et al., 2005; Cochrane, 2003; Andela et al., 2019), as is the fact that faster spread rates were observed in ecoregions that are generally non-forested (Massman et al., 2017; Andela et al., 2019). Because area burned estimates were derived from satellite instrumentation, some unburned islands were inevitably treated as burned (Kolden and Weisberg, 2007), and as is commonly reported in other data (Short, 2014), GlobFire data were observed to sometimes classify spatially distinct fire events as a single fire. These biases could result in models that overestimate individual fire spread rates, although the mean spread estimates from the Amazon ecoregion at least (0.44 km/day) did not dramatically differ from published ground-based estimates (Ray et al., 2005). It should be noted that the model parameters were estimated solely to minimize the RMSE. Consequently, the modeled growth curve sometimes extended beyond the observed duration of fire, so that although the growth curve matched the observations well, estimates of eventual burned area and duration from the model were too large. This phenomenon is important to keep in mind when interpreting the slight decrease in duration associated with high FDI values in the Amazon and Andean ecoregions (Figure 7). Because of these occasional counterintuitive predictions, we recommend that these models be primarily used to estimate spread rates, and that predictions of duration and eventual area burned be used with caution. The estimates of spread rates could be useful proxies for burnover risk and suppression effort for most ecoregions,

https://doi.org/10.5194/egusphere-2022-742
Preprint. Discussion started: 9 September 2022

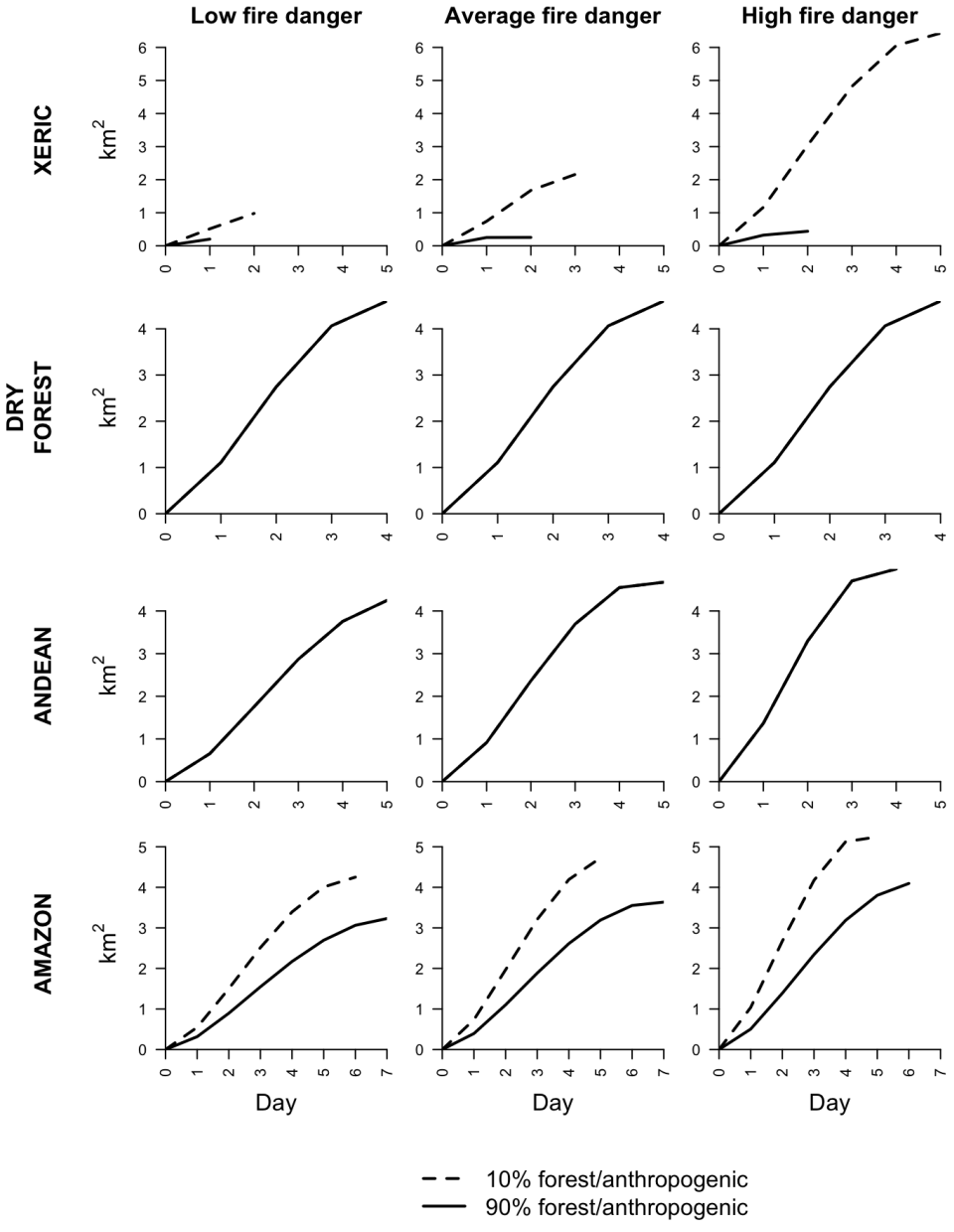

Figure 7. Expected daily burned area time series for each ecoregion under low fire danger (wettest 2% of days), normal fire danger (mean value of the relevant FDI), and dry (driest 2% of days) conditions, and at two extremes of the relevant land cover covariate.

but the Amazon may be somewhat of an exception. In the Amazon, the slow fire spread rates, low flame heights (Cochrane, 2003; Ray et al., 2005; Bufacchi et al., 2017), and sparse settlement suggest that explosive fire growth poses a practically

https://doi.org/10.5194/egusphere-2022-742
Preprint. Discussion started: 9 September 2022

non-existent threat to humans. Still, the Amazon should only very rarely have naturally occurring fire at all (Lima et al., 2012), and the spread model predictions might find use as a tool to identify when and where fire occurrence is possible.

4.2 Effects of meteorology and land cover on fire development

That fire spread was generally predicted to be higher during meteorological conditions considered conducive to fire spread is expected. And although the identification of the SC - which is interpreted as an estimate of idealized fire spread (Bradshaw et al., 1984) - as the best FDI in the Andean ecoregion is not surprising given that the ecoregion is generally non-forested, the fact that this same relationship was observed in the Amazon ecoregion was surprising. One might not expect that a FDI that was largely related to wind would be a useful proxy for fire spread in heavily forested and tropical ecosystems (Cochrane, 2003). However, the SC is not only computed from wind but also from the moisture content of the smaller fuel size classes (Bradshaw et al., 1984). It is therefore plausible that the SC was selected because, unlike the BI or ERC, it was a proxy of fuel moisture of lighter fuels that are characteristic of the Amazon's understory litter layer (Cochrane, 2003). These results also suggest that decision makers should reconsider their preferential use of other FDIs over the SC (Jolly et al., 2019), as the latter was the apparent best predictor of fire spread in multiple ecoregions (Table 3-4). The lack of a strong relationship between FDIs and fire spread in the dry forest and the weak relationship in the xeric ecoregion may also seem surprising. One explanation for this apparent lack of correlation in these two ecoregions is that the elevated human habitation in these locations relative to other portions of Peru reduces the effects of meteorology on fire spread, which is a phenomenon that has been observed in the United States (Syphard et al., 2017). Indeed, in the xeric ecoregion, anthropogenic cover had a weakly significant negative effect on fire spread (Table 3), suggesting that nearby human presence may dampen wildfire activity. Anthropogenic effects were less plausible explanatory variables in the Andean and Amazon ecoregions, which have relatively sparse human habitation[4], and the covariates used in the best-approximating models of these ecoregions reflect this fact (Table 3-4). Forest cover was a negative and very-strongly significant predictor of fire spread in the Amazon, which, as mentioned in the previous subsection, conforms with existing research regarding the global variability in fire spread rates (Andela et al., 2019).

In ecoregions where covariates were relevant, the observed relationships between the extinguish rates and the environment were sometimes counterintuitive. For instance, in the Andean and Amazon ecoregions, extinguish rates were positively related to FDIs, suggesting that drier conditions were conducive to fire extinguishment. The relationships between fire danger and extinguish rates are not easily dismissed as they are strongly significant (Table 4), and in the Amazon at least, we have fairly high confidence that the model is the best out of the 18 candidates (Figure 6). However, a satisfactory explanation for this counterintuitive result can be arrived at by revisiting the original mathematical model and observing the correlations between the two parameters. Consider that, as described at the end of subsection 2.2, the duration of the fire is controlled by the relative decay rate, which is the ratio of the spread rate and extinguish rate. This implies that the spread rate is proportional to the extinguish rate, with a harmonic number as the scalar. Here the scalar is a function of the fire's duration. We can then envision two ways that high covariance between the spread rates and extinguish rates can arise. First, if the variability in the duration is not too large, then the harmonic number scalars will not strongly vary. Second, if the average fire duration

[4]https://sedac.ciesin.columbia.edu/data/set/grump-v1-population-density/maps?facets=region:south%20america

https://doi.org/10.5194/egusphere-2022-742
Preprint. Discussion started: 9 September 2022

is large enough, then the harmonic number scalars will also not strongly vary. In any event, the mean and variance of the fire duration distributions resulted in spread rates and extinguish rates with high covariance, as is evidenced from the high spearman correlation coefficients and the strong fit of the quadratic models (Figure 4). It is then not surprising that similar models would arise for two parameters that are so closely correlated. Indeed, in the Amazon ecoregion, we can see that the exact same covariates are used in the extinguish rate model and the spread rate model (Table 3-4).

4.3 Future work

The results and methods in this paper provide a template for forecasting fire growth from environmental covariates. When a fire ignition is reported, estimates of the spread rate and extinguish rate can be calculated from environmental data, which would permit estimates of fire spread over time and secondarily of final size and duration over time. Future work might include additional covariates into these models to further improve predictive performance and by extension improve fire-related decisions. In addition to those explored in this paper, there are numerous other FDIs that could be included that might better model fire spread (Littell et al., 2016), with low-frequency FDIs potentially being of particular importance when modeling fire behavior in the more arid ecoregions in Peru (Meyn et al., 2007; Barbero et al., 2015b). Firefighting-related covariates could be used to forecast the effects various suppression strategies would have on fire behavior, and various ocean temperature indexes could be included to incorporate ENSO-related effects on fire spread (Chen et al., 2011; Block et al., 2000). Projected climatic and land use changes could be used to provide longer-term forecasts of fire risk and inform decisions such as firefighting staffing and training programs, as well as inform land management decisions. Future work should also explore the necessity of forecasting extinguish rates from environmental data or if these parameters may simply be inferred from predicted spread rates instead (Figure 4). Because the spatial domain of the GlobFire data covers the entire world, the methods described here can be readily applied to other ecoregions, which would be particularly useful to locations without access to sophisticated fire spread modeling capabilities. Future work may also seek to extend the principles governing this spatially-inexplicit difference equation model to spatially explicit fire spread models. Most fire spread occurs over a few days of a fire (Wang et al., 2017), and day-to-day variation in fire spread is an important variable for assessing burnover risk and, by extension, firefighting decision-making. Analysis of this day-to-day variability in fire spread was largely avoided in this analysis for practical reasons. Specifically, early exploratory analyses led us to expect that this task would present serious computational difficulties that are avoided with the simpler methods described in this paper. Nevertheless, this idea could be revisited in the future so that our simple model is extended to use daily forecasts of FDIs along with other covariates to explain day-to-day variation in fire spread. Although predictions from these models describe a time series of expected fire growth conditional on meteorological and land cover conditions, it is often the extreme fire events that are the most destructive and dangerous (Stephens et al., 2014; Viegas and Simeoni, 2011). These extreme events often occur in conditions that are unique to those that are typical of most other normal fires (Slocum et al., 2010; Barbero et al., 2015a) and are also likely the hardest to predict (Figure 5). For this reason, future work should validate the predictive performance of these models, with particular scrutiny paid to the times when extreme fires occur.

https://doi.org/10.5194/egusphere-2022-742
Preprint. Discussion started: 9 September 2022

5 Conclusions

In this paper, we developed a simple and intuitive difference equation model of fire growth that can be estimated using globally available satellite data. The difference equation was based on two parameters: the spread rate and the extinguish rate. We described the statistical distribution of these two parameters for four ecoregions in Peru using Gamma distributions. We also built generalized linear models to predict these parameters using FDI and land cover as covariates. We found that FDIs were statistically significant predictors of spread rates in the xeric, Andean, and Amazon ecoregions. We found that the SC was a strongly significant predictor of extinguish rates in the Andean ecoregion, and a very-strongly significant predictor in the Amazon ecoregion. In general, when FDIs were used to predict these two parameters, we found that the SC was usually the best choice, although model uncertainty was frequently high. On the other hand, model confidence was high in the Amazon ecoregion. In addition to FDIs, land cover was also a useful predictor in some contexts. Specifically, anthropogenic cover had a weakly significant and negative effect on spread rates in the xeric ecoregion, and forest cover had a very-strongly significant and negative effect on spread and extinguish rates in the Amazon ecoregion. Counterintuitive relationships were observed between extinguish rates and FDIs, where increased fire danger increased extinguish rates. These relationships were explained by the fairly strong correlation of the two model parameters. We argue that the methods presented here, although simple, are a promising method of forecasting fire spread risk for locations lacking access to sophisticated fire modeling capabilities.

Author contributions. conceptualization, H.R.P.; methodology, H.R.P. and W.M.J; software, H.R.P. and A.M.; validation, H.R.P. and W.M.J; formal analysis, H.R.P. and A.M.; investigation, H.R.P.; resources, E.A., and W.M.J; data curation, W.M.J and A.M.; writing–original draft preparation, H.R.P.; writing–review and editing, H.R.P., W.M.J, E.A., A.M., S.V., S.B.R., C.T.C., and B.P.V.; visualization, H.R.P. and S.B.R.; supervision, W.M.J and E.A.; project administration, H.R.P, B.P.V., W.M.J, and E.A.; funding acquisition, W.M.J and E.A.

Competing interests. The authors declare no competing interests.

Acknowledgements. This work was funded in part by the US Forest Service International Programs, the United States Agency for International Development, USFS Rocky Mountain Research Station, University of Washington, and the Fulbright Scholar Program. The authors would like to thank Isidoro Solis, Vannia Aliaga-Nestares, and Diego Rodriguez-Zimmermann.

https://doi.org/10.5194/egusphere-2022-742
Preprint. Discussion started: 9 September 2022

References

All, J., Medler, M., Arques, S., Cole, R., Woodall, T., King, J., Yan, J., and Schmitt, C.: Fire response to local climate variability: Huascarán National Park, Peru, Fire Ecology, 13, 85–104, 2017.

Andela, N., Morton, D. C., Giglio, L., Paugam, R., Chen, Y., Hantson, S., Van Der Werf, G. R., and Randerson, J. T.: The Global Fire Atlas of individual fire size, duration, speed and direction, Earth System Science Data, 11, 529–552, 2019.

Anderson, D. and Burnham, K.: Model selection and multi-model inference, Second. NY: Springer-Verlag, 63, 10, 2004.

Anderson, K. R., Englefield, P., Little, J., and Reuter, G.: An approach to operational forest fire growth predictions for Canada, International Journal of Wildland Fire, 18, 893–905, 2009.

Artés, T., Oom, D., De Rigo, D., Durrant, T. H., Maianti, P., Libertà, G., and San-Miguel-Ayanz, J.: A global wildfire dataset for the analysis of fire regimes and fire behaviour, Scientific data, 6, 1–11, 2019.

Barbero, R., Abatzoglou, J. T., Kolden, C. A., Hegewisch, K. C., Larkin, N. K., and Podschwit, H.: Multi-scalar influence of weather and climate on very large-fires in the Eastern United States, International Journal of Climatology, 35, 2180–2186, 2015a.

Barbero, R., Abatzoglou, J. T., Larkin, N. K., Kolden, C. A., and Stocks, B.: Climate change presents increased potential for very large fires in the contiguous United States, International Journal of Wildland Fire, 24, 892–899, 2015b.

Block, M., Richter, M., et al.: Impacts of heavy rainfalls in El Niño 1997/98 on the vegetation of Sechura Desert in Northern Peru (a preliminary report)., Phytocoenologia, 30, 491–517, 2000.

Bradshaw, L. S., Deeming, J. E., Burgan, R. E., and Cohen, J. D.: The 1978 National Fire-Danger Rating System: technical documentation, General Technical Report INT-169, U.S. Department of Agriculture, Forest Service, Intermountain Forest and Range Experiment Station., Ogden, UT, https://www.fs.fed.us/rm/pubs_int/int_gtr169.pdf, 1984.

Bufacchi, P., Santos, J. C., Veras, C. A. G., Alvarado, E. C., Mell, W., Carvalho, J. A., et al.: Probability of surface fire spread in Brazilian rainforest fuels from outdoor experimental measurements, European journal of forest research, 136, 217–232, 2017.

Butler, B. W.: Wildland firefighter safety zones: a review of past science and summary of future needs, International journal of wildland fire, 23, 295–308, 2014.

Chen, Y., Randerson, J. T., Morton, D. C., DeFries, R. S., Collatz, G. J., Kasibhatla, P. S., Giglio, L., Jin, Y., and Marlier, M. E.: Forecasting fire season severity in South America using sea surface temperature anomalies, Science, 334, 787–791, 2011.

Cochrane, M. A.: Fire science for rainforests, Nature, 421, 913–919, 2003.

Computing, R. et al.: R: A language and environment for statistical computing, Vienna: R Core Team, 2013.

De Vivo, F., Battipede, M., and Johnson, E.: Infra-red line camera data-driven edge detector in UAV forest fire monitoring, Aerospace Science and Technology, 111, 106 574, 2021.

Doerr, S. H. and Santín, C.: Global trends in wildfire and its impacts: perceptions versus realities in a changing world, Philosophical Transactions of the Royal Society B: Biological Sciences, 371, 20150 345, 2016.

Finney, M., Grenfell, I. C., and McHugh, C. W.: Modeling containment of large wildfires using generalized linear mixed-model analysis, Forest Science, 55, 249–255, 2009.

Fried, J. S. and Fried, B. D.: Simulating wildfire containment with realistic tactics, Forest Science, 42, 267–281, 1996.

Houtman, R. M., Montgomery, C. A., Gagnon, A. R., Calkin, D. E., Dietterich, T. G., McGregor, S., and Crowley, M.: Allowing a wildfire to burn: estimating the effect on future fire suppression costs, International Journal of Wildland Fire, 22, 871–882, 2013.

https://doi.org/10.5194/egusphere-2022-742
Preprint. Discussion started: 9 September 2022

Jolly, W. M., Freeborn, P. H., Page, W. G., and Butler, B. W.: Severe fire danger index: A forecastable metric to inform firefighter and community wildfire risk management, Fire, 2, 47, 2019.

Kolden, C. A. and Weisberg, P. J.: Assessing accuracy of manually-mapped wildfire perimeters in topographically dissected areas, Fire Ecology, 3, 22–31, 2007.

Lima, A., Silva, T. S. F., de Feitas, R. M., Adami, M., Formaggio, A. R., Shimabukuro, Y. E., et al.: Land use and land cover changes determine the spatial relationship between fire and deforestation in the Brazilian Amazon, Applied Geography, 34, 239–246, 2012.

Littell, J. S., Peterson, D. L., Riley, K. L., Liu, Y., and Luce, C. H.: A review of the relationships between drought and forest fire in the United States, Global change biology, 22, 2353–2369, 2016.

Massman, W. J., Forthofer, J., and Finney, M. A.: An improved canopy wind model for predicting wind adjustment factors and wildland fire behavior, Canadian Journal of Forest Research, 47, 594–603, 2017.

Melcher, T., Zinke, R., Trott, M., and Krause, U.: Experimental investigations on the repeatability of real scale fire tests, Fire Safety Journal, 82, 101–114, 2016.

Meyn, A., White, P. S., Buhk, C., and Jentsch, A.: Environmental drivers of large, infrequent wildfires: the emerging conceptual model, Progress in Physical Geography, 31, 287–312, 2007.

Nelder, J. A. and Mead, R.: A simplex method for function minimization, The computer journal, 7, 308–313, 1965.

Page, W. G., Freeborn, P. H., Butler, B. W., and Jolly, W. M.: A review of US wildland firefighter entrapments: trends, important environmental factors and research needs, International journal of wildland fire, 28, 551–569, 2019.

Podschwit, H., Guttorp, P., Larkin, N., and Steel, E. A.: Estimating wildfire growth from noisy and incomplete incident data using a state space model, Environmental and Ecological Statistics, 25, 325–340, 2018.

Price, O. F., Borah, R., and Maier, S. W.: Role of weather and fuel in stopping fire spread in tropical savannas, Austral Ecology, 39, 135–144, 2014.

Rapp, C. E., Wilson, R. S., Toman, E. L., and Jolly, W. M.: Assessing the role of short-term weather forecasts in fire manager tactical decision-making: a choice experiment, Fire Ecology, 17, 1–17, 2021.

Ray, D., Nepstad, D., and Moutinho, P.: Micrometeorological and canopy controls of fire susceptibility in a forested Amazon landscape, Ecological Applications, 15, 1664–1678, 2005.

Reed, W. J. and McKelvey, K. S.: Power-law behaviour and parametric models for the size-distribution of forest fires, Ecological Modelling, 150, 239–254, 2002.

Short, K.: A spatial database of wildfires in the United States, 1992-2011, Earth System Science Data, 6, 1–27, 2014.

Slocum, M. G., Beckage, B., Platt, W. J., Orzell, S. L., and Taylor, W.: Effect of climate on wildfire size: a cross-scale analysis, Ecosystems, 13, 828–840, 2010.

Stephens, S. L., Burrows, N., Buyantuyev, A., Gray, R. W., Keane, R. E., Kubian, R., Liu, S., Seijo, F., Shu, L., Tolhurst, K. G., et al.: Temperate and boreal forest mega-fires: Characteristics and challenges, Frontiers in Ecology and the Environment, 12, 115–122, 2014.

Sullivan, A. L.: Wildland surface fire spread modelling, 1990–2007. 2: Empirical and quasi-empirical models, International Journal of Wildland Fire, 18, 369–386, 2009a.

Sullivan, A. L.: Wildland surface fire spread modelling, 1990–2007. 1: Physical and quasi-physical models, International Journal of Wildland Fire, 18, 349–368, 2009b.

Syphard, A. D., Keeley, J. E., Pfaff, A. H., and Ferschweiler, K.: Human presence diminishes the importance of climate in driving fire activity across the United States, Proceedings of the National Academy of Sciences, 114, 13 750–13 755, 2017.

https://doi.org/10.5194/egusphere-2022-742
Preprint. Discussion started: 9 September 2022

Taylor, S. W., Woolford, D. G., Dean, C., and Martell, D. L.: Wildfire prediction to inform fire management: statistical science challenges, Statistical Science, 28, 586–615, 2013.

Twidwell, D., Wonkka, C. L., Sindelar, M. T., and Weir, J. R.: First approximations of prescribed fire risks relative to other management techniques used on private lands, PLoS one, 10, e0140 410, 2015.

Viegas, D. X. and Simeoni, A.: Eruptive behaviour of forest fires, Fire technology, 47, 303–320, 2011.

Wagenmakers, E.-J. and Farrell, S.: AIC model selection using Akaike weights, Psychonomic bulletin & review, 11, 192–196, 2004.

Wang, X., Parisien, M.-A., Taylor, S. W., Candau, J.-N., Stralberg, D., Marshall, G. A., Little, J. M., and Flannigan, M. D.: Projected changes in daily fire spread across Canada over the next century, Environmental Research Letters, 12, 025 005, 2017.

Wei, Y., Thompson, M. P., Belval, E., Gannon, B., Calkin, D. E., and O'Connor, C. D.: Comparing contingency fire containment strategies using simulated random scenarios, Natural Resource Modeling, 34, e12 295, 2021.

Zhong, X., Duckham, M., Chong, D., and Tolhurst, K.: Real-time estimation of wildfire perimeters from curated crowdsourcing, Scientific reports, 6, 1–10, 2016.

Appendix A: Q-Q plots

A0.1 Spread rate

A0.2 Extinguish rate

https://doi.org/10.5194/egusphere-2022-742
Preprint. Discussion started: 9 September 2022

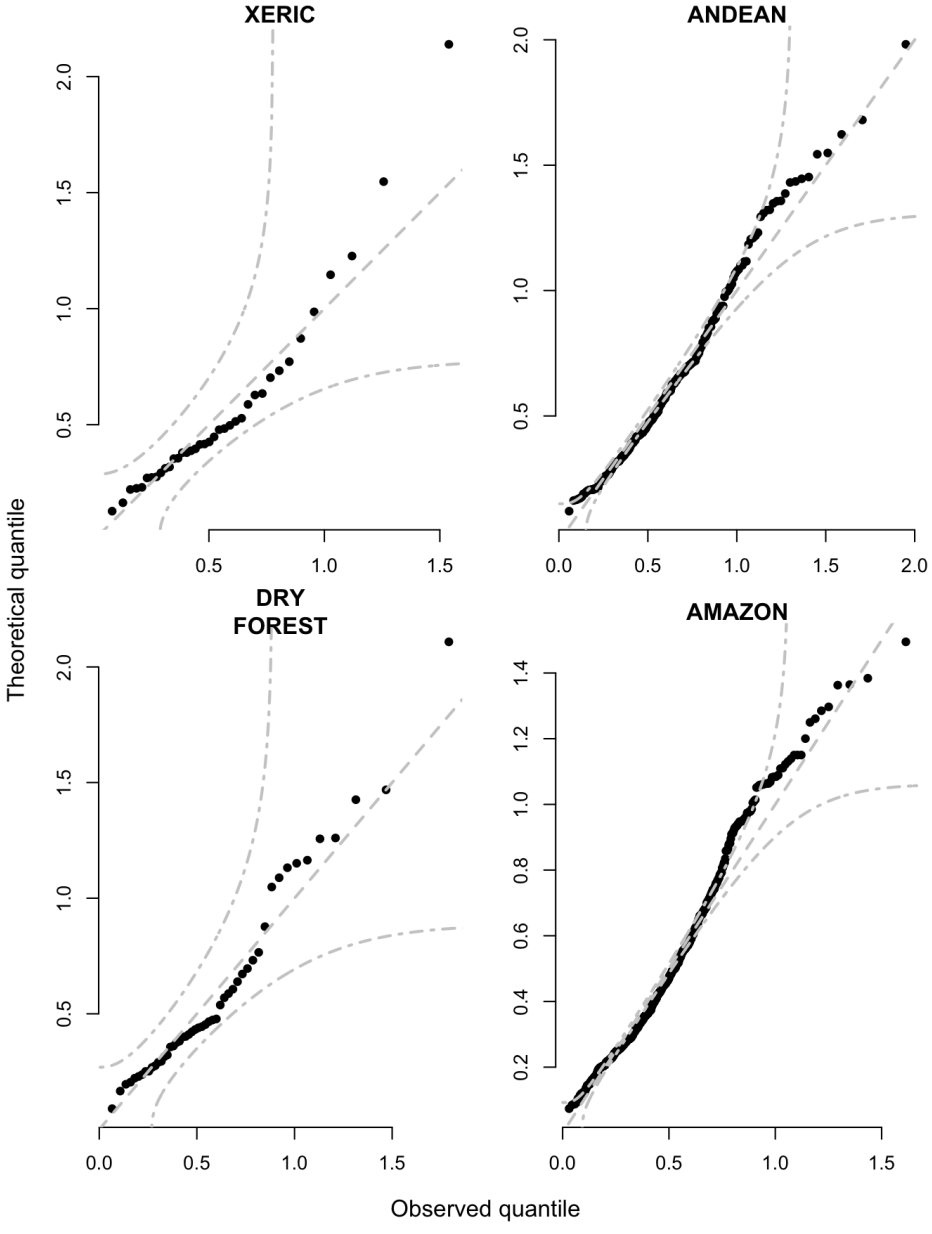

Figure A1. Q-Q plots of spread rate parameters disaggregated by ecoregion. 95% and median simultaneous confidence band shown in dashed lines.

https://doi.org/10.5194/egusphere-2022-742
Preprint. Discussion started: 9 September 2022

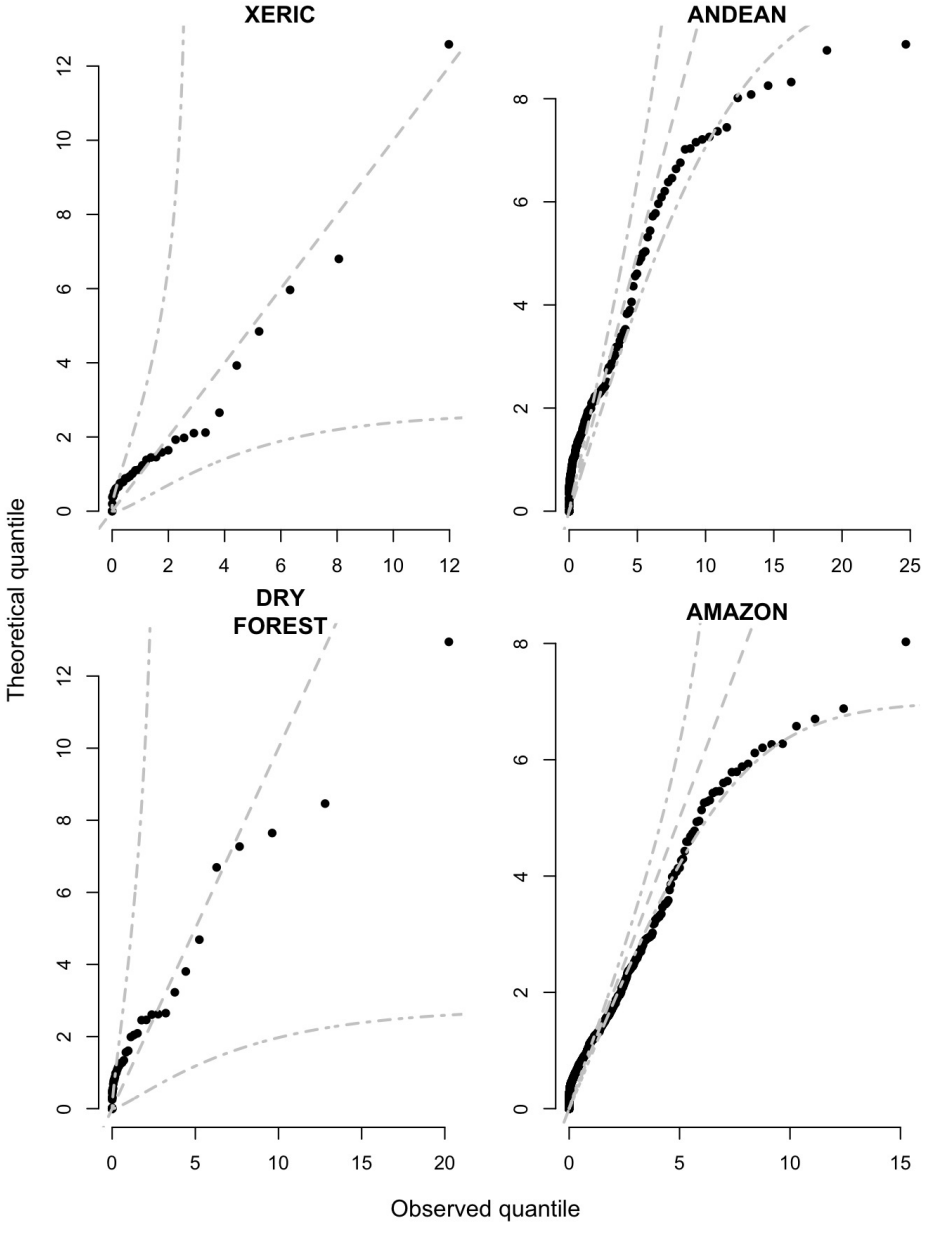

Figure B1. Q-Q plots of extinguish rate parameters disaggregated by ecoregion. 95% and median simultaneous confidence band shown in dashed lines.